Structure of light fields in natural scenes

Alexander A. Mury,[1] Sylvia C. Pont,[1,*] and Jan J. Koenderink[2]

[1]Delft University of Technology, Faculty of Industrial Design Engineering, Landbergstraat 15, 2628 CE Delft, The Netherlands

[2]Delft University of Technology, Faculty of Electrical Engineering, Mathematics and Computer Science, Mekelweg 4, 2828 CD Delft, The Netherlands

*Corresponding author: s.c.pont@tudelft.nl

Received 21 November 2008; revised 17 August 2009; accepted 23 August 2009; posted 24 August 2009 (Doc. ID 104366); published 25 September 2009

Light fields [J. Math. Phys. **18**, 51 (1936) ;*The Photic Field* (MIT, 1981)] of natural scenes are highly complex and vary within a scene from point to point. However, in many applications complex lighting can be successfully replaced by its low-order approximation [J. Opt. Soc. Am. A **18**, 2448 (2001); Appl. Opt. **46**, 7308 (2007)]. The purpose of this research is to investigate the structure of light fields in natural scenes. We describe the structure of light fields in terms of spherical harmonics and analyze their spatial variation and qualitative properties over scenes. We consider several types of natural scene geometries. Empirically and via modeling, we study the typical behavior of the first- and second-order approximation of the local light field in those scenes. The first-order term is generally known as the "light vector" and has an immediate physical meaning. The quadrupole component, which we named "squash tensor," is a useful addition as we show in this paper. The measurements were done with a custom-made device of novel design, called a "Plenopter," which was constructed to measure the light field in terms of spherical harmonics up to the second order. In different scenes of similar geometries, we found structurally similar light fields, which suggests that in some way the light field can be thought of as a property of the geometry. Furthermore, the smooth variation of the light field's low-order components suggests that, instead of specifying the complete light field of the scene, it is often sufficient to measure the light field only in a few points and rely on interpolation to recover the light field at arbitrary points of the scene.

OCIS codes: 120.5240, 150.2950.

1. Introduction

The quality of the light field, i.e., the directional properties of the illumination, strongly affects the appearance of an object positioned at that point [1–6]. For instance, in fully diffuse illumination even a specular metallic object looks rather matte. Diffuse illumination can very well have directional properties, for instance, the illumination from an overcast sky is directed vertically downward. However, the properties of diffuse and highly directional (collimated) illumination are very different. In collimated illumination, the shading is dominated by the presence of body and cast shadows, whereas in diffuse illumination shading gradients are much more gradual and much of the shading is actually due to vignetting. The surface structure of rough surfaces gives rise to texture in the case of collimated illumination, whereas it is hardly evident in the case of diffuse illumination. The light fields of natural scenes are often highly complicated functions; in general, the angular variations can be almost arbitrary, ranging from smooth (such as under an overcast sky) to very spiky (such as on a sunny day on the beach or the light patches in a forest) [7–11].

Because surface elements of a convex object are illuminated from half spaces, the surface irradiance is typically fairly smooth, even if the angular distribution of the radiance is spiky [1,2]. If the primary and secondary light sources are relatively distant from the region of interest, the spatial variations of the

0003-6935/09/285386-10$15.00/0

angular distribution will be minor over that region. Indeed, we have shown that although high-order properties of the light field vary rapidly over the scene (due to specularities, albedo variations, and so on), the low-order properties of the light field (ambient light, degree of diffuseness, primary direction of light, or what some artists call the "quality of light") stay rather constant as long as the geometry of the scene does not change much [12].

Gershun has introduced the very useful and intuitive notion of "light field" [13]. The light field is just the radiance as a function of location and direction. In computer graphics it is known as the plenoptic function [14]. At any point in space, the light field is a function of direction (spherical function). The radiance can be an almost arbitrary function of location and direction. Of course, it is nonnegative throughout. Another constraint is that in empty space the radiance in a certain direction does not change as one moves in that direction. In this paper, we are primarily interested in the illumination of diffusely scattering surfaces. The implication is that only the low-pass structure of the radiance is of importance [15]. This suggests that the Fourier description might be useful. For a spherical function, such as a light field, this comes down to spherical harmonics. A simple demonstration shows that the low orders of light fields in natural scenes change rather smoothly and systematically over the scene: if we take a matte convex object and move it around the scene, its appearance changes slowly except for points that are close to large objects (like a wall) or that occlude a large part of the primary illumination. In this paper we address the question of how the structure of the light field varies over the scene and what the relation is between the scene geometry and the quality of light in that scene.

We analyze the structure of light fields in terms of spherical harmonics and consider the structural properties up to the second order. It has been shown that this allows sufficiently accurate quantitative description of the shading of Lambertian surfaces [15]. For heuristic purposes, it is useful to consider the qualitative structure of the zeroth-, first- and second-order terms in the spherical harmonic development individually. The spherical harmonic development is usually known as a multipole development in physical context. The zeroth order is represented by the monopole (a scalar) and describes the "ambient light" of computer graphics. The first order is represented by the dipole contribution. The dipole transforms as a vector, it is the light vector as defined by Gershun. The light vector describes the transportation of radiant energy through surface elements. The second order describes the quadrupole contribution. Gershun does not explicitly discuss this order of approximation. The translators of Gershun's classical paper, Moon and Timoshenko, already mentioned "The light field considered in this book is a classical three-dimensional vector field. But the physically important quantity is actually the illumination, which is a function of five independent variables, not three. Is it not possible that a more satisfactory theory of the light field could be evolved by use of modern tensor methods in a five-dimensional manifold? We must look to the mathematician for any such development" [13]. In this paper we develop an intuitive notion of the quadrupole field as the "squash tensor" taking a first step in such a development.

The monopole contribution describes a constant illumination from all directions. This is usually known as ambient illumination in computer graphics [16], or Ganzfeld illumination in psychology. Formally, the monopole contribution at a given point is simply the average radiance over all directions. From a physical perspective, it describes the local volume density of radiation, measured in terms of photon density or total ray length per unit volume. An operational definition simply uses a spherical photocell or a translucent spherical shell with a photosensor in its interior [13]. Light fields in which the monopole contribution dominates are rare in nature. An example is an overcast sky over a snow cover, giving rise to "polar white-out."

The dipole contribution describes a unidirectional light field. Because the radiance is nonnegative, pure dipole fields cannot be implemented. The combination of a monopole and a dipole term yields what is known as the "point source at infinity with ambient term" of computer graphics [16]. Formally, the light vector describes the net transport of radiant power [13]. Thus, the transport of radiant power can be visualized by way of the field lines of the "light vector." These field lines do not coincide with the light rays, for instance, they can be curved and even closed. In empty space, the light field has zero divergence. The light vector can be measured by way of a back-to-back sandwich of two planar photocells. Their difference signal yields the component of the light vector in the direction of the surface normal. A natural light field that approximates a dipole dominated light field is the overcast sky. A simple approximation that is often useful is the hemispherical diffuse source.

The quadrupole contribution transforms as a symmetric traceless tensor. An operational definition similar to the photocell sandwich suggested by Gershun for the dipole component can be based on a cube with flat photocells as faces. To measure the quadrupole one has to search for the canonical orientation (see below). A simpler way to measure the quadrupole tensor involves radiance measurements for a larger number of directions. In that case, the instrument can be used in any orientation. We describe such a instrument in this paper. Quadrupole dominated light fields occur in the case of ring sources or two-point sources at opposite sides of the region of interest [17,18]. We refer to the quadrupole field as the squash tensor [12], which describes the geometry of these configurations.

The light field at a certain location in a scene depends both on the location, magnitude, and directional properties of the primary light sources and on

the geometry and scattering properties of the environment (for examples see Fig. 1). The influence of the geometry is twofold. One important effect is the obstruction of the primary illumination. In highly directional light fields, one speaks of body and cast shadows, in more general cases, in which sources can be partially occluded; the effect is known as vignetting. The other effect is due to multiple scattering between different, even remote, parts of the scene. This effect is sometimes known as "interreflection" or "reflexes." Both vignetting and interreflections depend strongly on the geometry of the scene. Since the radiation balance is described by a linear integral equation of the Fredholm type [19], the variance effects can be decoupled. The so-called pseudofacets depend only on the scene, not on the primary sources. In some cases the resulting light field is almost purely due to the geometry. An example of a geometry-dominated effect due to vignetting is the general low irradiance of surfaces inside concavities, for instance, the eye sockets in a face illuminated by an overcast sky are usually dark. An example of a geometry-dominated effect due to interreflection is the integrating sphere. The light field in the interior will be monopole-dominated irrespective of the primary sources. The contribution of the reflected light to the global light field is usually less significant than the primary illumination (due to the fact that albedo in natural scenes is rather low, and besides, the materials in natural scenes are mostly matte, therefore the reflected light is rather diffuse) but still yield a noticeable effect.

The global layouts of the scenes can vary a lot depending on the environment. A generic example is an open landscape, which is also the simplest one—the light field consists of the primary illumination, which is coming from the upper hemisphere and constant everywhere over the scene (due to the absence of objects that may occlude the primary light), and a diffuse reflected beam from the ground, which can vary over the scene due to albedo variation. The light field in such a scene is almost constant everywhere. A more complex type is the forest scene—here the primary illumination is due to the light that comes through openings in the foliage, and therefore the local light fields are very "spiky." The high orders vary a lot over such a scene, however the low-order properties are rather stable (these properties of course depend on the weather condition and the density of the foliage)—the dominant illumination direction is primarily from above, and the ambient component does not change much either. Urban scenes in general are more structured. However, one can distinguish certain patterns of geometric layouts, which are very typical, for instance, wall, street, and, for indoor scenes, room profiles. In these cases, the primary illumination is due to the visible part of sky, which varies systematically with the location in the scene. The regularity in geometry suggests that the low-order components of the light field would vary in a systematic manner as well. The reflective properties of materials present in the scene define scattering and interreflections. The exact angular distributions of the material reflectances are less important (though the albedos are). Taking into account the major role of scene geometry and smooth variation of the low orders, we expect that in scenes of similar geometric layouts one should expect to find qualitatively similar low-order light fields. In that sense, the light field can be thought of as a property of the geometry.

To test our hypothesis, we measured low-order components (light density, light vector, and the squash tensor) of light fields in natural scenes. We considered simple and frequently found in nature street, wall, and room geometries in different illumination conditions. We also developed simple models of these scenes and found a strong correspondence between real measurements and our simplified models.

For measurements, we used a custom-made device which we named a "Plenopter," which is designed to measure light fields up to the second order in terms of spherical harmonics. To the best of our knowledge, the light measuring devices currently available on the market are capable of measuring the structure of local light fields only up to the first order. Measuring light fields up to the second order is a useful addition in the analysis of the structure of light fields,

Fig. 1. From left to right, a matte convex object under a collimated source from above on a black, absorbing ground (vertically oriented dipole) and on a white ground causing a secondary source from below (combination of vertically oriented dipole and quadrupole). Next the object was illuminated by collimated sunlight from the left plus ambient light (monopole plus almost horizontally oriented dipole) and with a white screen at the right causing a secondary source from the right (monopole plus almost horizontally oriented dipole and quadrupole).

because the squash tensor is a significant characteristic of natural light fields. Therefore, we believe that our measurement device forms a major innovation in this field. In addition to the main goal of this investigation, we summarize the technical details of the design of our measurement system.

2. Theory

The concept of "the light field" was introduced by Gershun in the 1930s. Gershun considers the scalar field of radiation volume density and the vector field of net flux propagation. Gershun's "light vector" $\mathbf{D}$ is defined such that, for any oriented surface element dA, the net flux $d\Phi = \mathbf{D} \cdot dA$, where the sign indicates the direction of net flux propagation. The formal properties of Gershun's light field were further developed by Moon and Spencer [20]. In this paper, we extend the formalism to include second-order properties of the light field.

The light field is defined by Gershun as essentially a low-order approximation to the radiance. The radiance is a function of position and direction that completely describes the luminous environment. Gershun's scalar field is the zeroth order and Gershun's vector field the first-order approximation to the radiance. This is essentially the initial part of a development of the radiance in terms of spherical harmonics.

A. Second Order Properties of the Light Field

The local light field at a fixed point in space is a spherical function (radiance as a function of direction) $f(\vartheta, \varphi)$ and can be represented as the sum of its harmonics:

$$f(\vartheta, \varphi) = \sum_{l=0}^{\infty} \sum_{m=-l}^{l} f_{l,m} Y_{l,m}(\vartheta, \varphi). \tag{1}$$

The real-valued basis functions are defined as

$$Y_{l,m}(\vartheta, \varphi) = \begin{cases} \sqrt{2} K_{l,m} \cos(m\varphi) P_{l,m}(\cos\vartheta), & m > 0, \\ \sqrt{2} K_{l,-m} \sin(-m\varphi) P_{l,-m}(\cos\vartheta), & m < 0, \\ K_{l,0} P_{l,0}(\cos\vartheta), & m = 0, \end{cases} \tag{2}$$

where the $P_{l,m}$ are the associated Legendre polynomials and $K_{l,m}$ are normalization factors.

Spherical harmonics form an orthonormal basis on the unit sphere. Coefficients $f_{l,m}$ can be calculated as

$$f_{l,m} = \int_{\varphi=0}^{2\pi} \int_{\vartheta=0}^{\pi} f(\vartheta, \varphi) Y_{l,m}(\vartheta, \varphi) \sin(\vartheta) \mathrm{d}\vartheta \mathrm{d}\varphi. \tag{3}$$

One has $l \geq 0$ and $-l \leq m \leq l$. Thus, order l consists of $2l + 1$ basis functions. In the rotations of the coordinate system, the coefficients transform for each order individually, that is to say, the orders do not "mix." Therefore, the radiance can be represented as a sum of its components of different orders. The zeroth order represents Gershun's scalar field and the first-order Gershun's vector field. Any order l can be represented as a list of corresponding coefficients $SH_l(f) = \{f_{l,-l}, f_{l,-l+1}, \ldots, f_{l,l}\}$, and the representation of the entire function is a combination of the orders, i.e., $SH(f) = \{SH_0(f), SH_1(f), SH_2(f), \ldots\}$.

The *monopole* component, that is the zeroth-order term $\mathbf{M} = \{2\sqrt{\pi} f_0\}$, corresponds to Gershun's "density of light" or "space illumination." It is essentially the average radiance. The monopole term is a fundamental property of the light field that describes the overall illumination at a point, i.e., how much radiance arrives at a point from all directions. From a computer graphics point of view, the zero order term can be thought of as an "ambient component."

The *dipole* component, that is the first-order term $\mathbf{D} = \{f_{1,-1}, f_{1,0}, f_{1,1}\}$ transforms as a vector. This vector corresponds to Gershun's "light vector"—the direction of maximum energy transfer at the point under consideration. The projection of the light vector on any direction results in flux density in that direction. Rotating the dipole in such a way that it is aligned with the z axis, it can be represented as $\mathbf{D}^{\mathrm{rot}_d} = \{0, 0, v\}$, where $v = 2\sqrt{\frac{\pi}{3}} \sqrt{f_{1,-1}^2 + f_{1,0}^2 + f_{1,1}^2}$ is the magnitude of the light vector. From a computer graphics point of view, the first-order term can be thought of as a diffuse directional beam.

The *quadrupole* component, that is the second-order term $\mathbf{Q} = \{f_{2,-2}, f_{2,-1}, f_{2,0}, f_{2,1}, f_{2,2}\}$, consists of five basis functions. Under rotations, these components transform as a symmetric tensor of trace zero. We refer to it as the "squash tensor." By a suitable rotation, any quadrupole can be represented as $\mathbf{Q}^{\mathrm{rot}_q} = \{0, 0, q^+, 0, q^-\}$. The two coefficients q^+ and q^- represent basis functions $f_{2,0}$ and $f_{2,2}$ and completely describe the structure (quality) of the squash tensor.

By a suitable rotation of the axis, the spherical harmonic development can be reduced to a convenient canonical form. We consider two possibilities. In case the dipole dominates the squash tensor (the generic case), a convenient canonical form is

$$\begin{aligned} SH_2^{\mathrm{rot}_d}(LF) &= \{\mathbf{M}^d, \mathbf{D}^d, \mathbf{Q}^d\} \\ &= \{\{d_0\}, \{0, 0, v\}, \{f_{2,-2}^d, f_{2,-1}^d, f_{2,0}^d, f_{2,1}^d, f_{2,2}^d\}\}. \end{aligned} \tag{4}$$

In this case we require seven coefficients. The remaining two degrees of freedom are absorbed by the rotation of the axes. In case the squash tensor dominates the dipole (at singular points of the vector field), it is more convenient to use the canonical representation:

$$\begin{aligned} SH_2^{\mathrm{rot}_q}(LF) &= \{\mathbf{M}^q, \mathbf{D}^q, \mathbf{Q}^q\} \\ &= \{\{d_0\}, \{f_{1,-1}^q, f_{1,0}^q, f_{1,1}^q\}, \{0, 0, q^+, 0, q^-\}\}. \end{aligned} \tag{5}$$

In this case, we need only six coefficients, the remaining three degrees of freedom being absorbed by the rotation of the axes. Of these six coefficients, only the three that define the monopole and squash tensor will be significant and $f^q_{1,-1}$, $f^q_{1,0}$, and $f^q_{1,1}$ will be close to zero. The structure can be represented graphically as shown in Fig. 2.

B. Physical Interpretation of the Squash Tensor

The monopole component d_0, the dipole component $v = \{f^q_{1,-1}, f^q_{1,0}, f^q_{1,1}\}$, and the squash tensor component specified by q^+ and q^- are rotationally invariant descriptors of the structure of the light field. The physical meaning of the squash tensor component is most easily grasped in the case that the light vector vanishes. Because the radiance is a nonnegative function of direction, the monopole component is always necessary. There are two qualitatively different configurations for such a pure quadrupole field. One is the "light clamp" (therefore "squash tensor"), which corresponds to the light field between two identical light sources opposite to each other. The other configuration is that of a "light ring" (Fig. 3).

3. The Plenopter

We have constructed a device that makes it possible to measure the light field up to (and including) the second order as a single observation. The device is roughly spherical with a diameter of 20 cm. It can easily be taken outdoors to do measurements in a natural environment. Instead of using cameras with fish-eye lenses, we used a number of photodiodes. This greatly expands the dynamic range at the cost of spatial resolution. We took our inspiration from a number of devices proposed by Gershun. Gershun's device for the observation of the light vector consists of a sandwich of photocells in a back-to-back configuration. This device is very similar to ours except for the fact that Gershun divides the sphere into two, while we divide into 12 congruent apertures.

L \ M	-2	-1	0	1	2
0			0.282		
1		-0.063	0.226	-0.040	
2	-0.018	-0.012	0.099	-0.066	0.045

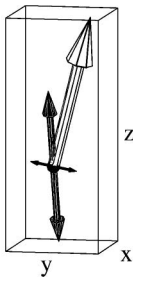

Fig. 2. Schematic graphical representation of the second-order light field. The SH coefficients are presented on the left side. The mutual orientation of the components D, $q+$, and $q-$ is shown on the right side. The length of the light gray arrow corresponds to the value d_1 (strength of the light vector), the lengths of the dark gray and black arrows correspond to values $q+$ and $q-$. Note that these dark gray and black arrows are perpendicular to each other and that there are always two dark gray and two black arrows opposite each other, together representing a quadrupole (two positive and two negative poles perpendicular to each other).

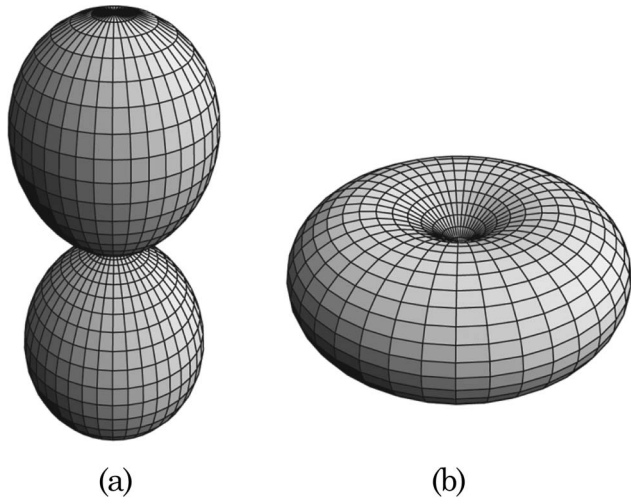

Fig. 3. Special cases of light fields due to the squash tensor: (a) a light clamp and (b) a light ring. The light vector is assumed to be zero.

A. Short Description

The second-order development in spherical harmonics contains nine free parameters. The simplest regular polyhedron with nine or more faces is the dodecahedron, which has 12 faces. The sphere of directions was divided into 12 mutually congruent pentagonal solid angles. The photocells collect radiation from these apertures, which have a diameter of 2× 74.75°. Diaphragms and a diffuser were placed so as to uniformly integrate over the aperture. The photocells were Siemens BPW21 silicon photodiodes (sensitive from 350 to 820 nm) connected to logarithmic amplifiers followed by an AD converter. We obtain a dynamic range of about seven decades. A single observation thus yields 12 radiance samples. From this overdetermined sample, we find the coefficients of the spherical harmonic development by means of a least squares method. Currently the remaining three degrees of freedom are discarded.

B. Basic Data Conversion

A single plenopter measurement yields 12 values corresponding to the 12 photocells. The photocells have a certain angular sensitivity profile $S_j(\theta, \phi)$ as a function of the direction of the incident light $LF_j(\theta, \phi)$.

Thus,

$$P_j = \int S_j(\theta, \phi) \cdot LF(\theta, \phi) d\Omega, \qquad j = 1, \ldots, 12, \quad (6)$$

where P_j is the output value corresponding to cell j.

The photocells' angular sensitivity profile was measured and decomposed to spherical harmonics, so it can be represented as

$$S_j(\theta, \phi) = \sum_{lm} s^j_{l,m} \Upsilon_{l,m}(\theta, \phi) + \varepsilon^j. \quad (7)$$

The shape of the sensitivity profile is the same for all photocells (but may differ by a scaling factor), so

once the profile for one of the cells has been measured, all the others can be achieved by rotation and scaling. Furthermore, we can describe the radiance in terms of spherical harmonics as

$$LF(\theta,\phi)=\sum_{lm}c_{l,m}\Upsilon_{l,m}(\theta,\phi)+\varepsilon. \tag{8}$$

In the sequel, we neglect the errors ε. Then, altogether, this results in

$$\begin{aligned}P_j&=\int[\sum_{lm}s^j_{l,m}\Upsilon_{l,m}(\theta,\phi)][\sum_{l'm'}c_{l',m'}\Upsilon_{l',m'}(\theta,\phi)]\mathrm{d}\Omega\\&=\sum_{ll',mm'}s^j_{l,m}c_{l',m'}\int\Upsilon_{l,m}(\theta,\phi)\Upsilon_{l',m'}(\theta,\phi)\mathrm{d}\Omega\end{aligned} \tag{9}$$

and, due to orthonormality of spherical harmonics basis functions

$$\int\Upsilon_{l,m}(\theta,\phi)\Upsilon_{l',m'}(\theta,\phi)=\delta_{l,l'}\delta_{m,m'}, \tag{10}$$

we finally end up with

$$P_j=\sum_{lm}s^j_{l,m}v_{l,m}=(\vec{s^j},\vec{c}). \tag{11}$$

If we renumber the coefficients and limit the spherical harmonics approximations to the second order (i.e., $l=0,..,2$, $m=-l,..l$ altogether nine coefficients), we get a system of 12 equations with nine unknowns, c_k:

$$P_j=\sum_{k=1}^{9}s^j_kc_k. \tag{12}$$

The system is overdetermined, and an approximate solution can be found by means of a least squares technique [21]. The plenopter is 120° rotation symmetric, therefore we can get more data for that system rotating the plenopter around its vertical axis. The angular sensitivity profiles for the cells in their new orientations can be achieved rotating the spherical harmonics description $S_j(\theta,\phi)$. Each rotation adds 12 more equations to the system providing more data.

C. Calibration and Tolerances

The basic photoelectric calibration was done in a calibrated solar simulator using a set of calibrated neutral density filters.

There are many processes that lead to systematic and random errors. We investigated the following:

— thermal properties, drift, offset, etc., of the 12 photoelectric subsystems;
— deviations from a curved logarithmic response for the individual subsystems;
— the spectral sensitivities of the subsystems;
— the precise geometry of the apertures of the subsystems;
— possible issues of optical and electrical cross talk.

We used standard methods to investigate these possible issues. We find a mixture of minor systematic and random errors. In the final analysis, the instrument can be said to yield correct results within about 5% if no special corrections are applied. This was judged to be sufficient for the current application.

The sample frequency is at least 100 Hz. The experiments reported here were essentially static though.

4. Empirical Light Field Studies

In the general introduction, we hypothesized that the light field can be thought of as a property of the scene geometry. Here we describe empirical studies in which we tested this hypothesis by modeling and measuring light fields of a few canonical scene geometries. For negative edge (a long street) and step (a long wall adjacent to a large square) geometries, we compared measurements at several points along and across the streets and walls. We did measurements in three typical narrow streets and one square in the old part of Utrecht. The streets were about 10 m wide, and the buildings alongside the street and square were about 10 m high. Measurements were taken with a step size of approximately 1 m at a height of 1.5 m. We tested under clear sky and under overcast sky conditions, so the primary light sources were the Sun (if not occluded) and the visible part of sky (which forms a stripe). If our hypothesis is right, the measurements along the streets and walls should be constant up to minor nonsystematic differences, while those across the streets and walls should change systematically and smoothly. Second, we modeled these qualitative aspects of the second-order approximations.

To demonstrate the influence of albedo we also compared measurements and models for an indoor scene with a black and with a white wall. For this purpose, we used a laboratory room 6×5 m with a window on the wide side and matte black side walls and ceiling, facing North. So, here the primary light source was only the part of the sky that was visible through the window. We considered two situations: the long wall opposite the window was covered by white or black paper. Measurements were taken over a 3×3 points grid at a height of 1.5 m, 1.5 m apart in one direction and 1.25 m apart in the other direction.

A complete set of measurements took about 15 min per scene. The coefficients of the second-order spherical harmonic approximations (SH2) were estimated by the overdetermined system described in Section 3, via least squares optimization.

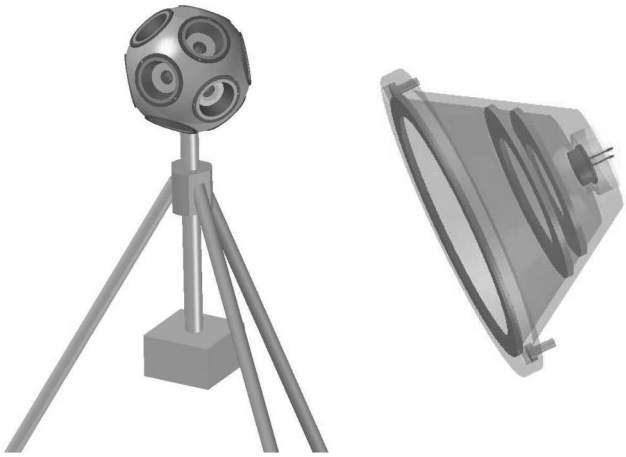

Fig. 4. Our custom-made light measuring device which we named "Plenopter."

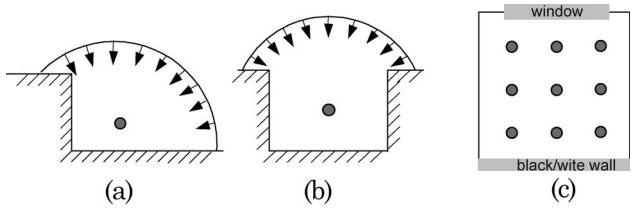

Fig. 5. Schematic descriptions of the scenes: (a) wall, (b) street, and (c) room.

A. Models

For the street and wall scenes we made schematic representations; see Fig. 5. The width of the street and the height of the walls were measured in the real scenes where the measurements were taken. The walls were assumed to be uniform and infinitely long. The position of the Sun and the orientation of the street with respect to the Sun were looked up on the basis of the geographic coordinates and measurement times and dates.

The primary illumination in our scenes was due to the Sun and sky. For the description of the radiance distribution from the sky and Sun, we used International Commission on Illumination (CIE) standard models [22]; in the case of a clear sky we used the "CIE standard clear sky, low illuminance turbidity," and in the case of an overcast sky model, the "overcast, moderately graded and slight brightening towards the Sun" model.

Taking into account the low spatial resolution of the second-order light field [12], we assume that their properties can be sufficiently captured by very simple models. A second-order approximation can be thought of as a low frequency filter which filters out high frequencies introduced by specularities and small albedo variations. Therefore, the material properties do not have to be specified in detail. For simplicity we assume them to be Lambertian and

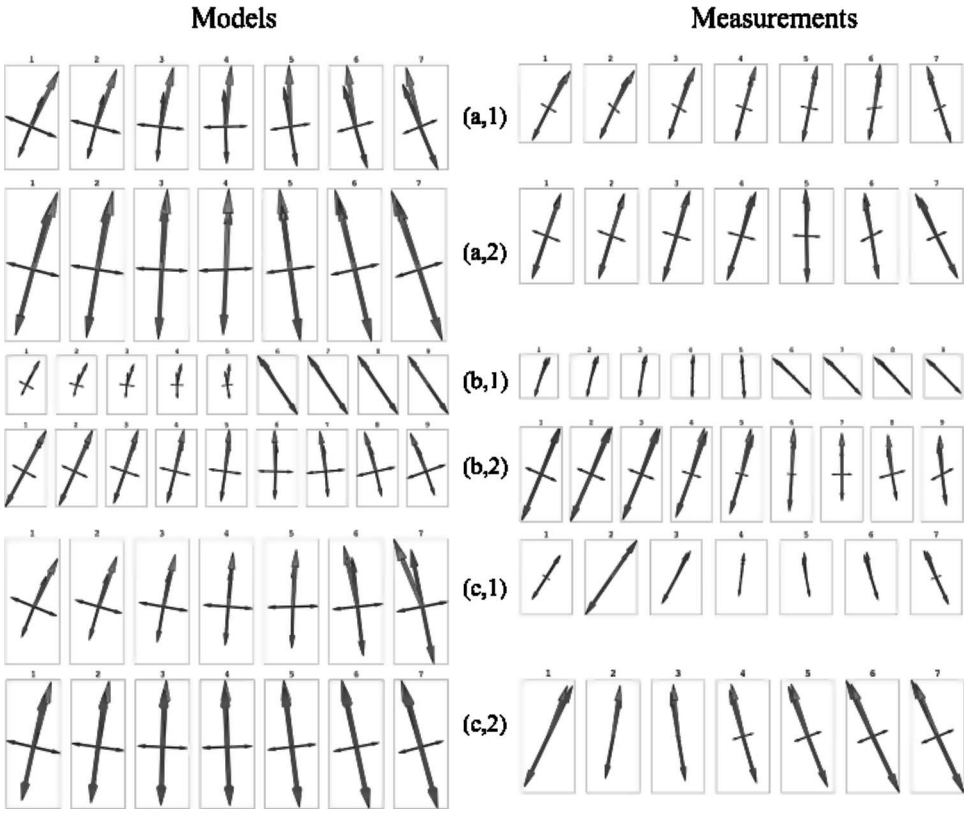

Fig. 6. Comparison of models (left) and measurements (right) for street scene configurations, for three streets (a), (b) and (c) in (1) clear and (2) overcast sky conditions. The vectors represent the light field up to the second order (see Figure 2). We considered from seven to nine points per scene (depending on the scene dimensions).

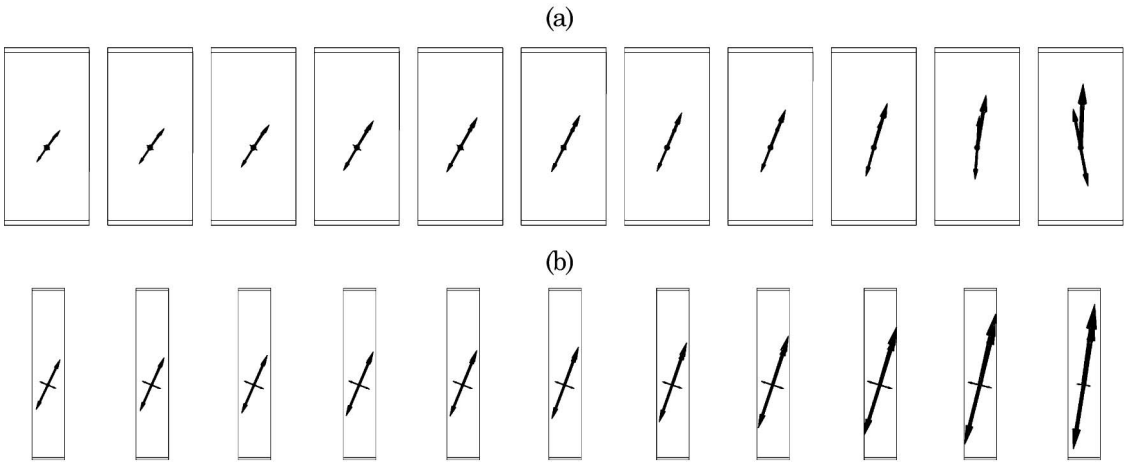

Fig. 7. Measurements of second-order light fields for the wall scene in the case of (a) a clear sky and (b) an overcast sky. The Sun was not visible in either case.

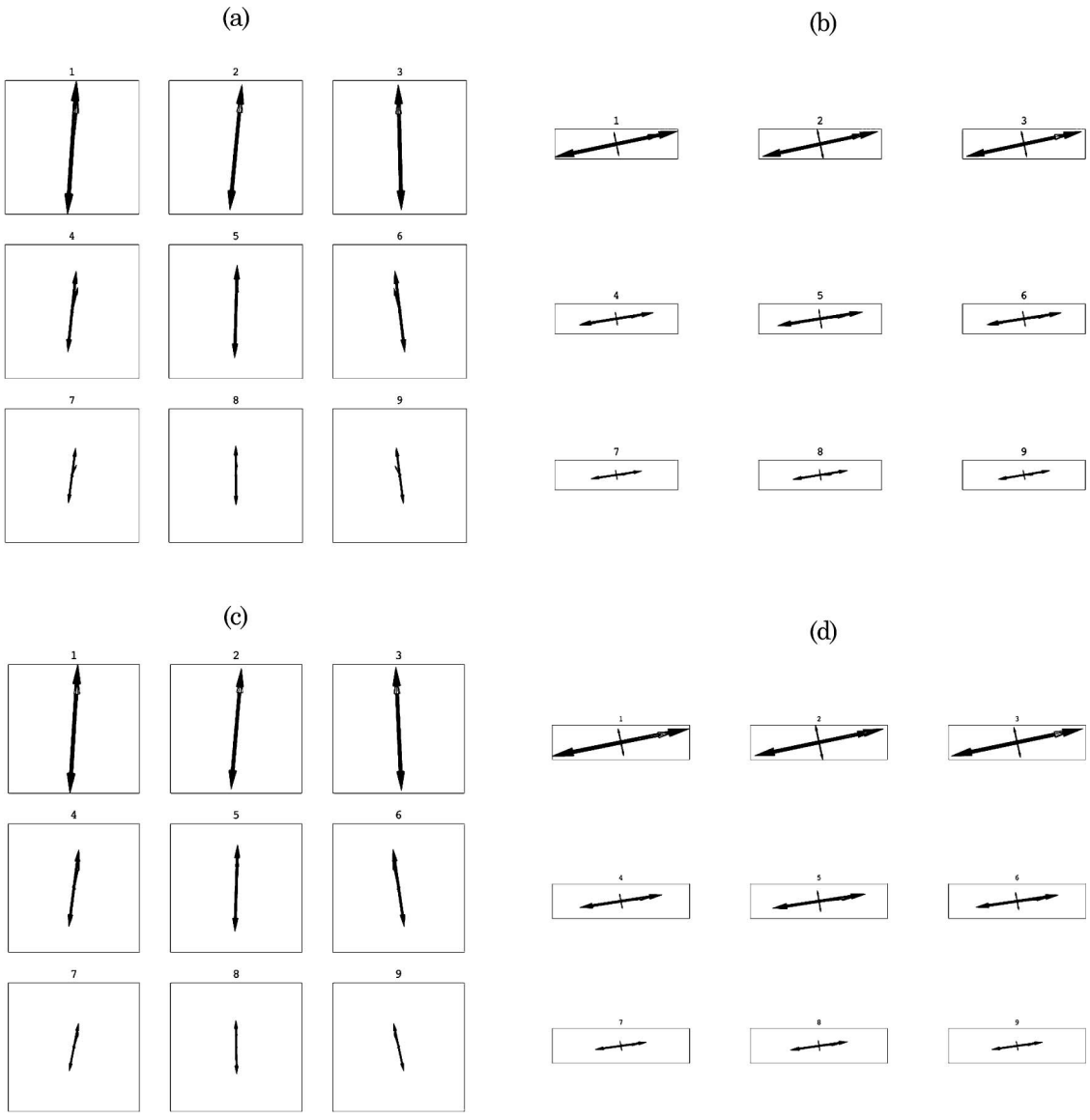

Fig. 8. Measurements for the room scene: (a) and (b) white wall; (c) and (d) black wall; (a) and (c) view from above; (b) and (d) view from a side.

uniform with albedo 0.1, which is an average albedo for urban scenes [23] (note: the models were found to be robust for small variations of the albedo).

The models were implemented in Mathematica 5.2. We took into account up to two interreflections.

B. Results

The second-order light fields for the street geometries are shown in Fig. 6. On the left side, we show the predictions from the models, on the right side the actual measurements. The spherical harmonics coefficients for each point were normalized (scaled) by the DC component at that point to allow comparisons between points and between models and measurements. The results for the three streets (a), (b), and (c) in clear sky (1) and overcast sky (2) conditions are depicted in different rows. In (b,1) the Sun was directly visible from points 6–9. In all other cases the Sun was occluded either by clouds or by buildings. In Fig. 6 we clearly see that, first, the measurements change smoothly and systematically as a function of position in the scene; second, the global structures of the light fields are similar for the measurements and simple models; third, the global structures of the light fields are similar for the different streets.

Figure 7 shows the measurements for the wall geometry. The top row shows results for a clear sky; the bottom row for an overcast sky. The Sun was not directly visible in neither cases. Here we also see smooth and systematic behavior of the light field. In Figs. 6 and 7 we can see a clear difference between overcast and clear sky conditions. Under a clear sky the light vector is stronger and aligned with the positive component of the quadruple, whereas the negative component of the squash tensor is quite small. However, in the case of an overcast sky the negative component of the squash tensor becomes larger (the light field is more diffuse).

Figure 8 shows the measurements for the room scene of which the wall opposite to the window was matte white [(a) and (b)], or matte black [(c) and (d)]. In the left half, we depicted views from above [(a) and (c)], and in the right half side views [(b) and (d)] of individual measurements. The window was located near points 1–3. The results for the white and black walls look very similar, however the magnitudes of the light vectors and the squash tensors show clear and systematic differences, especially at the points that are closer to the back wall; see Fig. 9: the absorption of the black wall results in a relatively stronger dipole component.

5. Discussion

The measurements clearly indicate that, in scenes of similar geometry, the light fields demonstrate characteristic variations of the light vector and the squash tensor over the scene. This happened despite the fact that the streets possessed different reflective properties and even were differently oriented with regard to the primary light sources (the Sun). So

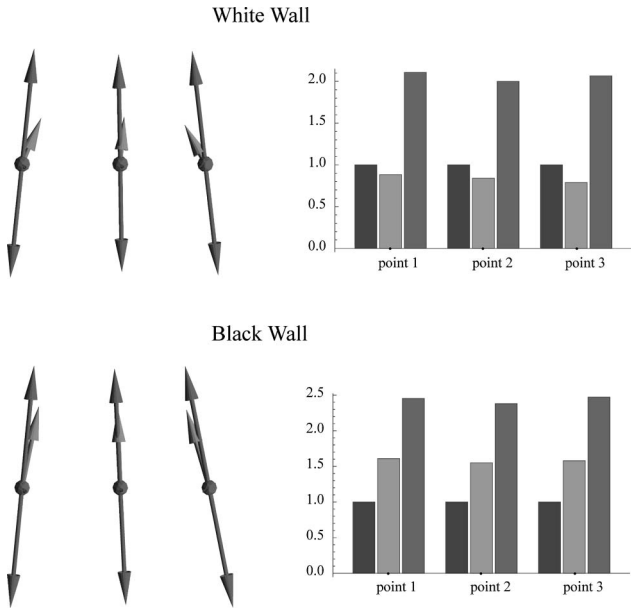

Fig. 9. Room scene: At the left we show the vector representations for the points near the wall for the white and the black cases. At the right we show the ratios of the magnitudes of the mono-, di-, and quadruples with the monopole.

these results are in line with our hypothesis that in scenes of similar geometrical layouts one should expect to find qualitatively similar low-order light fields and, in that sense, the light field can be thought of as a property of the geometry.

Although there are some deviations between our simple model predictions and the actual measurements, the correspondence between them is evident. The main difference concerns the negative components of the –approximately horizontally oriented– quadruples which tend to be larger in the theoretical predictions than in the measurements for the wall and street scenes. This may be due to the fact that in the models we assumed the materials to be Lambertian and uniform, while real materials may scatter light in different ways. For example, backscattering of rough surfaces [24] or (off-)specular scattering tends to result in angular distributions of the scattered radiance that are centered around the illumination direction and specular direction, respectively. In combination with a primary light source from above, this may result in a relatively smaller contribution from reflections of the walls and therefore smaller quadruples.

The measurements in the room scene (Fig. 8) confirm that the secondary light sources are much less significant than the primary illumination and geometry. The main differences between the white and black wall conditions concern the points that are just next to the wall. Note that in real scenes albedo variations usually are much less extreme. Thus, the smooth and systematic behavior of the low orders over the scene suggests that similar patterns may be found in any other scene with a similar geometry (assuming the light comes only from the window).

We have presented a new technique to capture the global structure of the light field in terms of spherical harmonical functions. Existing techniques to capture the light field, the photic field, the plenoptic function, or the Lumigraph [25] result in representations with a much higher angular resolution. These techniques are very useful for high-quality renderings of scenes that include small and glossy objects. However, our technique is sufficient for scenes with large matte objects and provides a potentially very high spatial resolution; the number of points at which plenopter measurements are taken may be very high—individual measurements including placement of the apparatus just take a minute. Moreover, it provides this high spatial resolution in combination with an extreme high dynamic range up to 7 decades; note that simple photographic techniques can never cover this dynamic range. Moreover, our technique provides insight into the global structure of light fields. This may help to understand what, for instance, a "natural complex light field" [7–10] actually means and to check whether the hypotheses about it ([26–29]) are true. These insights into the global structure of natural light fields are important for fields that involve the perceptual qualities of the illuminance environment, such as architecture, interior design, and illumination engineering.

This work was supported by the Netherlands Organization for Scientific Research (NWO). We thank Ruurd Lof and the Debye Institute (Utrecht University) for use of their solar simulator. We thank all the technicians of the Science Instrumentation workplace and Hans Kolijn (Utrecht University) for working out the design of and actually building the Plenopter.

References

1. C. Cuttle, *Lighting by Design* (Architectural Press, 2003).
2. C. Cuttle, "Lighting patterns and the flow of light," Light. Res. Technol. **3**, 171–189 (1971).
3. L. Michel, *Light: the Shape of Space* (Wiley, 1995).
4. T. S. Jacobs, *Drawing with an Open Mind* (Watson-Guptill, 1991).
5. M. Baxandall, *Shadows and Enlightenment* (Yale University, 1995).
6. A. Adams, *The Negative* (Little, Brown and Company, 1981).
7. R. O. Dror, T. K. Leung, E. H. Adelson, and A. S. Willsky, "Statistics of real-world illumination," in *Proceedings of the IEEE Computer Society Conference on Computer Vision and Pattern Recognition* (IEEE, 2001), pp. 164–171.
8. R. W. Fleming, R. O. Dror, and E. H. Adelson, "Real-world illumination and the perception of surface reflectance properties," J. Vision **3**, 347–368 (2003).
9. R. O. Dror, A. S. Willsky, and E. H. Adelson, "Statistical characterization of real-world illumination," J. Vision **4**, 821–837 (2004).
10. J. Huang and D. Mumford, "Statistics of natural images and models," in *Computer Vision and Pattern Recognition* (IEEE, 1999), pp. 541–547.
11. S. Teller, M. Antone, M. Bosse, S. Coorg, M. Jethwa, and N. Master, "Calibrated, registered images of an extended urban area," in *Proceedings of the IEEE Conference on Computer Vision and Pattern Recognition* (IEEE, 2001), pp. 93–107.
12. A. A. Mury, S. C. Pont, and J. J. Koenderink, "Light field constancy within natural scenes," Appl. Opt. **46**, 7308–7316 (2007).
13. A. Gershun, "The light field," J. Math. Phys. **18**, 51–151 (1936) (translated by P. Moon and G. Timoshenko).
14. E. H. Adelson and J. R. Bergen, "The plenoptic function and the elements of early vision," in *Computational Models of Visual Processing*, M. Landy and J. A. Movshon, eds. (MIT, 1991), pp. 3–20.
15. R. Ramamoorthi and P. Hanrahan, "On the relationship between radiance and irradiance: determining the illumination from images of a convex Lambertian object," J. Opt. Soc. Am. A **18**, 2448–2459 (2001).
16. J. D. Foley, A. van Dam, S. K. Feiner, and J. F. Hughes, *Computer Graphics, Principles and Practice* (Addison Wesley, 1990).
17. C. J. Copi, D. Huterer, D. J. Schwarz, and G. D. Starkman, "On the large-angle anomalies of the microwave sky," Mon. Not. R. Astron. Soc. 1–27 (2005).
18. M. R. Dennis and K. Land, "Probability density of the multipole vectors for a Gaussian cosmic microwave background," Mon. Not. R. Astron. Soc. **383**(2), 424–434 (2007).
19. J. J. Koenderink and A. J. van Doorn, "Geometrical modes as a general method to treat diffuse interreflections in radiometry," J. Opt. Soc. Am. **73**, 843–850 (1983).
20. P. Moon and D. E. Spencer, *The Photic Field* (MIT, 1981).
21. W. H. Press, S. A. Teukolsky, W. T. Vetterling, and B. P. Flannery *Numerical Recipes in C* (Cambridge University, 1988).
22. S. Darula and R. Kittler, "CIE General Sky standard defining luminance distributions," in *Proceedings ESim Conference* (IBPSA, 2002), pp. 1113.
23. H. Akbari, L. S. Rose, and H. Taha, "Characterizing the fabric of the urban environment: a case study of Sacramento, California," LBNL-44688, Lawrence Berkeley National Laboratory, Berkeley, California, 1999.
24. S. C. Pont and J. J. Koenderink, "Reflectance from locally glossy thoroughly pitted surfaces," Comput. Vision Image Understand. **98** (2), 211–222 (2005).
25. S. J. Gortler, R. Grzeszczuk, R. Szeliski, and M. F. Cohen, "The lumigraph," in *Computer Graphics (SIGGRAPH96) Proceedings* (ACM, 1996), pp. 43–54.
26. H. M. Fox and G. Vevers, *The Nature of Animal Colours* (Sidqwick and Jackson, 1960).
27. D. Gomez and M. Thery, "Simultaneous crypsis and conspicuousness in color patterns: comparative analysis of a neotropical rainforest bird community," Am. Nat. **169**, S42–S61 (2007).
28. G. H. Thayer, *Concealing Coloration in the Animal Kingdom* (Macmillan, 1909/1918).
29. J. A. Endler, "The color of light in forests and its implications," in *Ecological Monographs 63* (Ecological Society of America, 1993), pp. 1–27.